



DALHOUSIE UNIVERSITY

Retrieved from DalSpace, the institutional repository of
Dalhousie University

<https://dalspace.library.dal.ca/handle/10222/79598>

Version: Post-print

Publisher's version: Whittleton, Sarah; Otero de la Roza, Alberto; J. Johnson, Erin. (2017). The exchange-hole dipole dispersion model for accurate energy ranking in molecular crystal structure prediction. *Journal of Chemical Theory and Computation*, 13, 441-450. <https://doi.org/10.1021/acs.jctc.6b00679>

The exchange-hole dipole dispersion model for accurate energy ranking in molecular crystal structure prediction

Sarah R. Whittleton,[†] A. Otero-de-la-Roza,[‡] and Erin R. Johnson^{*,†}

Department of Chemistry, Dalhousie University, 6214 Coburg Road, Halifax, Nova Scotia, Canada B3H 4R2, and Department of Chemistry, University of British Columbia, Okanagan, 3247 University Way, Kelowna, British Columbia, Canada V1V 1V7.

E-mail: erin.johnson@dal.ca

Abstract

Accurate energy ranking is a key facet to the problem of first-principles crystal-structure prediction (CSP) of molecular crystals. This work presents a systematic assessment of B86bPBE-XDM, a semilocal density functional combined with the exchange-hole dipole moment (XDM) model, for energy ranking using 14 compounds from the first five CSP blind tests. Specifically, the set of crystals studied comprises 11 rigid, planar compounds and 3 co-crystals. The experimental structure was correctly identified as the lowest in lattice energy for 12 of the 14 total crystals. One of the exceptions is 4-hydroxythiophene-2-carbonitrile, for which the experimental structure was correctly identified once a quasi-harmonic estimate of the vibrational free-energy contribution was included, evidencing the occasional importance of thermal corrections for accurate energy ranking. The other exception is an organic salt, where charge-transfer error (also called delocalization error) is expected to cause the base density functional to be unreliable. Provided the choice of base density functional is appropriate and an estimate of temperature effects is used, XDM-corrected density-functional theory is highly re-

liable for the energetic ranking of competing crystal structures.

Introduction

One of the continuing scandals in the physical sciences is that it remains impossible to predict the structure of even the simplest crystalline solids from a knowledge of their composition.

J. Maddox, Crystals from first principles. *Nature*, **1988**, 335, 201.

First-principles crystal-structure prediction (CSP) is a grand challenge in computational chemistry. Current approaches have shown promise for small molecules, with limited flexibility and some *a priori* knowledge of the crystal structure, such as the number of molecules in the asymmetric unit.¹⁻⁵ However, there is presently no general, reliable way to predict the complex three-dimensional crystal structure of an arbitrary compound from its molecular structure.⁶ CSP protocols essentially consist of three distinct steps, each posing difficulties of their own: i) the efficient generation of sensible candidate crystal structures for the molecule under study, ii) the screening of these candidates to arrive at a short list of relatively stable structures, and iii) the accurate calculation of their free energy differences to determine the

*To whom correspondence should be addressed

[†]Dalhousie University

[‡]University of British Columbia

thermodynamically stable structure. The second and third step may use the same methodology, but it is also possible to use a more accurate (and more computationally expensive) method for the final ranking. In this work, we focus on this third step.

The problem of energy ranking of molecular crystal structures is intimately related to polymorphism.⁷⁻¹⁰ Polymorphism in molecular crystals is particularly relevant to the pharmaceutical industry since different polymorphs will have different physical properties, such as solubilities, that can affect their bioavailability.¹¹⁻¹⁴ The case of the drug ritonavir¹⁵ illustrates the importance of determining the stable form of active pharmaceutical ingredients. Additionally, polymorphism impacts the development of energetic materials because differences in crystal structure will affect their thermal stability and sensitivity to shock.^{16,17} Polymorphism is also key in the design of thin films and organic electronics since the crystal packing will affect their charge-transfer efficiency.¹⁸⁻²⁰

To assess the performance of different CSP protocols, the Cambridge Crystallographic Data Centre (CCDC) periodically holds blind-test competitions.¹⁻⁵ In these tests, unpublished experimental X-ray crystal structures are obtained for a small number of organic compounds. The molecular diagram of these compounds are announced and research groups have a period of one year to submit their top three candidate crystal structures, which are then compared to the experimental result. To date, there have been six blind tests, organized in 1999,¹ 2001,² 2004,³ 2007,⁴ 2010,⁵ and 2016.²¹ In this work, we focus on compounds from the first five blind tests, which will be labeled as BT1 to BT5 in the rest of the article.

In the previous blind tests, the vibrational and entropic effects are generally assumed to be minor,²² and the crystal structures with lowest electronic energy are commonly taken to be the most thermodynamically favourable. Nyman and Day²³ recently demonstrated that thermal effects can change the identity of the most stable candidate structure for about 9% of compounds, based on a computational com-

parison of the energies for 1061 experimental structures of 508 organic molecules. A further largely unavoidable assumption is that the experimentally-observed structure is indeed the thermodynamically stable phase, which may or may not be the case.²⁴

Most groups participating in the published blind tests use force-field methods to rank candidate crystal structures using either atomic charges or a distributed-multipoles force field, with empirical R^{-6} dispersion terms. Neumann *et al.*²⁵ participated in the last two blind tests (CSP2007⁴ and CSP2010⁵) and obtained good results using dispersion-corrected density-functional theory.²⁶ Brandenburg and Grimme have also recently assembled a benchmark for organic-crystal energy ranking using the compounds from the sixth blind test.²⁷

DFT methods have been shown to provide good results for polymorph ranking in oxalyl dihydrazide,^{28,29} p-diiodobenzene,³⁰ glycine,³¹ pyrazinamide,³² and ice.³³ In all cases, the energy differences between isolable polymorphs are necessarily quite small, nearing degeneracy.³⁴ In recent years, the applicability of DFT to molecular crystals has greatly increased, thanks to the development of dispersion corrections that can be paired with popular base density functionals. These include Grimme's D2 and D3 methods,^{35,36} the non-local van der Waals density functional (vdW-DF),^{37,38} the Tkachenko-Scheffler³⁹ and the more-recent many-body dispersion (MBD) model,⁴⁰ and the exchange-hole dipole moment (XDM) model,⁴¹⁻⁴³ co-developed by one of us. The XDM method has been shown to yield excellent accuracy for sublimation enthalpies of molecular crystals⁴⁴ and for the calculation of the enantiomeric excess of a solution at the chiral eutectic.⁴⁵

The XDM⁴⁴ method, as well as others,⁴⁶⁻⁴⁸ has demonstrated good performance in the calculation of absolute lattice energies of molecular crystals on standard benchmark sets.⁴⁴ In this work, we take a different approach and assess the performance of XDM (specifically, the B86bPBE-XDM functional) for energy ranking of molecular crystals using the blind-test structures as our benchmark data set. The calcu-

lated XDM-corrected energies for the top three crystal structures submitted by each group are compared with the energy for the experimental structure. As in previous blind tests, we assume that the experimental structure is given the electronic energy minimum. We consider only rigid, planar molecules, or co-crystals of two rigid molecules, which limits the study to 14 out of a total of 21 compounds from the first five blind tests. B86bPBE-XDM predicts the experimental structure to be lowest in energy for 12 of 14 compounds, while the 13th requires that thermal effects are taken into account through calculation of the free energy differences. The remaining exception is the organic salt, for which good performance is not expected due to the inherent charge-transfer (delocalization) error⁴⁹⁻⁵⁴ of the base density functional. Overall, B86bPBE-XDM is shown to be a viable method for accurate energy ranking of molecular crystal structures, with a computational cost that is essentially the same as any other periodic GGA crystal geometry relaxation. Hence, it is a very good option for the final ranking step in a CSP protocol.

Computational Methods

All crystal structures were obtained from the supplementary information of the previous published blind tests.¹⁻⁵ Only the three most stable structures from each method that were submitted to the blind test competition were considered. Full geometry relaxations were performed for all crystals with the B86bPBE^{55,56} density functional and the XDM dispersion correction.^{41,42} B86bPBE-XDM has shown excellent performance in the calculation of absolute⁴² and relative⁴⁵ lattice energies of molecular crystals, as well as in the modeling of more exotic non-covalent interactions, such as adsorption on metal surfaces.⁵⁷

B86bPBE-XDM has the correct asymptotic exchange enhancement factor behavior in the limit of large reduced density gradient, and is therefore expected to give an accurate representation of three-body (three-molecule) exchange-repulsion and induction effects.⁵⁴ Errors in the

intermolecular three-body energy term (particularly when using the PBE functional) are typically much higher than non-additive three-molecule dispersion contributions.⁵⁴ In consequence, although an extension of XDM including Axilrod-Teller-Muto dispersion terms is available,⁵⁸ we use the canonical pairwise implementation of XDM. It should be also noted that the XDM dispersion coefficients are dependent on properties of the electron density through the exchange hole multipole moments. This means that the dispersion coefficients are quite sensitive to changes in chemical environment^{57,59} and, due to this density dependence, XDM implicitly accounts for non-additive many-atom effects on the dispersion coefficients in a similar fashion to the MBD approach.⁴⁰

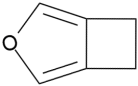
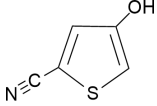
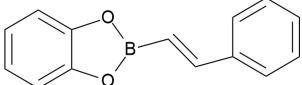
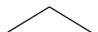
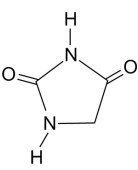
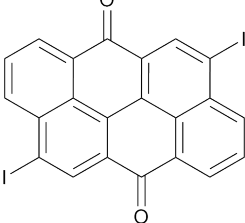
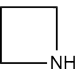
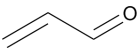
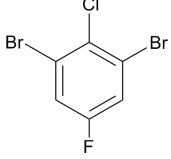
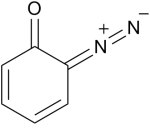
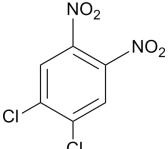
All calculations used the periodic-boundary, plane-wave/pseudopotentials approach and the Projector Augmented Wave (PAW) formalism⁶⁰ with either version 4.3.2 (modified to include XDM⁴²) or version 5.1.2 of the Quantum Espresso program.⁶¹ An 80 Ry plane-wave cutoff, an 800 Ry density cutoff, and a $4\times 4\times 4$ Γ -centered \mathbf{k} -point grid were used in all cases. Initial calculations used the default convergence criteria, but to resolve the small energy differences between structures, further calculations with tighter convergence criteria of 10^{-5} Ry on the energy and 10^{-4} Ry/bohr on the forces were performed for structures found to be less than 0.4 kcal/mol higher in energy than the experimental structures. Atomic charges for the organic salt were calculated using the Yu-Trinkle algorithm⁶² within the critic2 program.⁶³

Results and Discussion

Single-Molecule Crystals

The results for the 11 single-molecule crystals are summarized in Table 1. The notation chosen follows the blind test nomenclature, where the structures are identified by the last names of one member of the participating groups and either 1, 2, or 3 to indicate the rank within that group’s three submitted structures. The cal-

Table 1: Summary of XDM-corrected and base density-functional results for the single-molecule crystals. The blind test (“BT”) in which the crystal structures were reported is indicated, and the roman numeral is the compound identifier in the blind test articles. The ✓ symbol indicates that the experimental crystal structure was correctly predicted to be the lowest in energy. The ✗ symbol indicates that at least one other polymorph was predicted to be lower in energy than the experimental structure. The difference in energy between the most stable candidate and the experimental structure is also shown with and without XDM (ΔE_{XDM} and ΔE_{base} , both in kcal/mol). The latter was calculated at the B86bPBE-XDM equilibrium geometry.

Compound	Number	BT	XDM	Base	ΔE_{XDM}	ΔE_{base}
	I	1	✓ ^a	✗	—	-0.30
	II	1	✗	✓	-0.26	—
	III	1	✓	✗	—	-2.21
	VII	1	✓	✗	—	-0.30
	VIII	3	✓	✗	—	-0.19
	IX	3	✓	✗	—	-0.34
	XI	3	✓	✗	—	-0.07
	XII	4	✓	✗	—	-0.11
	XIII	4	✓	✗	—	-0.47
	XVI	5	✓	✓	—	—
	XVII	5	✓	✓	—	—

^aTwo experimental polymorphs were identified for this compound.¹ Energies and volumes are reported relative to form 1, predicted to be more stable by 0.17 kcal/mol with DFT-XDM.

culated energies for each structure, relative to experiment, are also shown graphically in Figure 1, with and without the XDM dispersion correction.

The DFT-XDM approach is found to correctly predict the experimental crystal structure as the energy minimum for all but one of the compounds considered in Table 1. Conversely, the base functional alone (at the DFT-XDM geometry) only predicts the experimental structure to be lowest in energy for three compounds (II, XVI, and XVII). Figure 1 shows that, in absence of the dispersion correction, the base functional predicts many structures to be more stable than the experimental crystal—some of them by as much as 2 kcal/mol. In all the cases where the base functional fails, a lower-density structure is predicted to be more stable (data given in the SI). This is to be expected since dispersion typically favours more dense packing, so neglect of dispersion should favour lower-density structures. A similar re-ranking of structures when a dispersion correction is applied has been reported by Braun *et al.*^{64,65} Interestingly, the authors show that energy ranking is sensitive to the type of dispersion correction at the DFT level, indicating the need of benchmarking results for dispersion corrected DFT methods.

Neumann and co-workers participated in the BT4 and BT5 using dispersion-corrected DFT together with a system-specific potential fitted to reproduce dispersion-corrected DFT results for each compound.²⁶ Specifically, they used the PW91 functional^{66,67} and an empirical dispersion correction based on the work of Wu and Yang⁶⁸ that involves a pairwise sum over C_6 terms only. The C_6 coefficients were obtained by fitting to reproduce molecular dispersion coefficients. Changes in C_6 with chemical environment⁵⁹ are taken into account using explicit atom typing according to hybridization.²⁶ Neumann *et al.* correctly predicted the experimental structure for all four of the single, planar-molecule crystals considered (XII, XIII, XVI, XVII). The similar, excellent performance of both this methodology and DFT-XDM implies that ranking lattice energies of molecular crystals is an easier prob-

lem for dispersion-corrected DFT compared to computing accurate lattice energy differences.⁴⁵ Given the considerable difference between Neumann *et al.*'s and B86bPBE-XDM methodological approaches, we conclude that the results for the present set of compounds do not appear to be particularly sensitive to the choice of base functional or the form of the dispersion correction.

In the remainder of this section, details regarding the crystal structures of the compounds in Figure 1 and Table 1 are discussed at length. First, the structure of compound I (the rigid molecule from BT1 with only C, H, N, and O¹) was correctly predicted by four participants (Verwer-1, Williams-1, Gavezzotti-1, and van Eijck-3) and is identified as the minimum-energy structure by B86bPBE-XDM. Compound I is particular in that a second polymorph (with space group $P2_1/c$), different from the blind test target ($Pbca$) has been determined, a fact that was unknown at the time the blind test contest was held, but discussed in the subsequent article.¹ None of the other methods applied were successful in ranking the $P2_1/c$ structure as close in energy to $Pbca$, even though the candidate was often generated, and many groups point to the inadequacy of the employed force fields.¹ B86bPBE-XDM predicts the $P2_1/c$ polymorph to be 0.17 kcal/mol higher in energy than $Pbca$ (blue line in Figure 1), which is within the ± 1 kJ/mol typical energy range for isolable polymorphs proposed by Nyman and Day²³ (in the following, the “polymorphism energy range”). The remaining structure shown in red in Figure 1 is van Eijck-3, which was identified as correct in the blind test but, when relaxed using B86bPBE-XDM, converges to a slightly different equilibrium structure where the molecules are displaced with respect to one another along the molecular plane. Given the small energy difference, the two minima are likely interconvertible when crystal vibrations are taken into account.

The only single crystal where DFT-XDM predicts a structure to be more stable than experimental is compound II, 4-hydroxythiophene-2-carbonitrile. This case is complicated by the fact that, in a occurrence similar to what is

Figure 1: Relative DFT-XDM energies for all submitted structures, ordered by blind test (blocks marked as 1, 3, 4, 5) in kcal/mol per molecule. The experimental structure is taken as the zero of energy in both plots. The top figure shows the dispersion-corrected (black) and uncorrected (purple) energies. The shaded region (± 1 kJ/mol around zero) represents the typical energy differences between isolable polymorphs.²³ The bottom plot shows the dispersion-corrected energies in a smaller region around zero. The red lines correspond to candidate structures that are not observed experimentally. The energies for the experimental structures are shown in green. Blue lines are alternative experimental structures: for compound I, the blue line is the energy for the second observed polymorph ($P2_1/c$); for compound XXI, the blue lines correspond to different proton orderings.

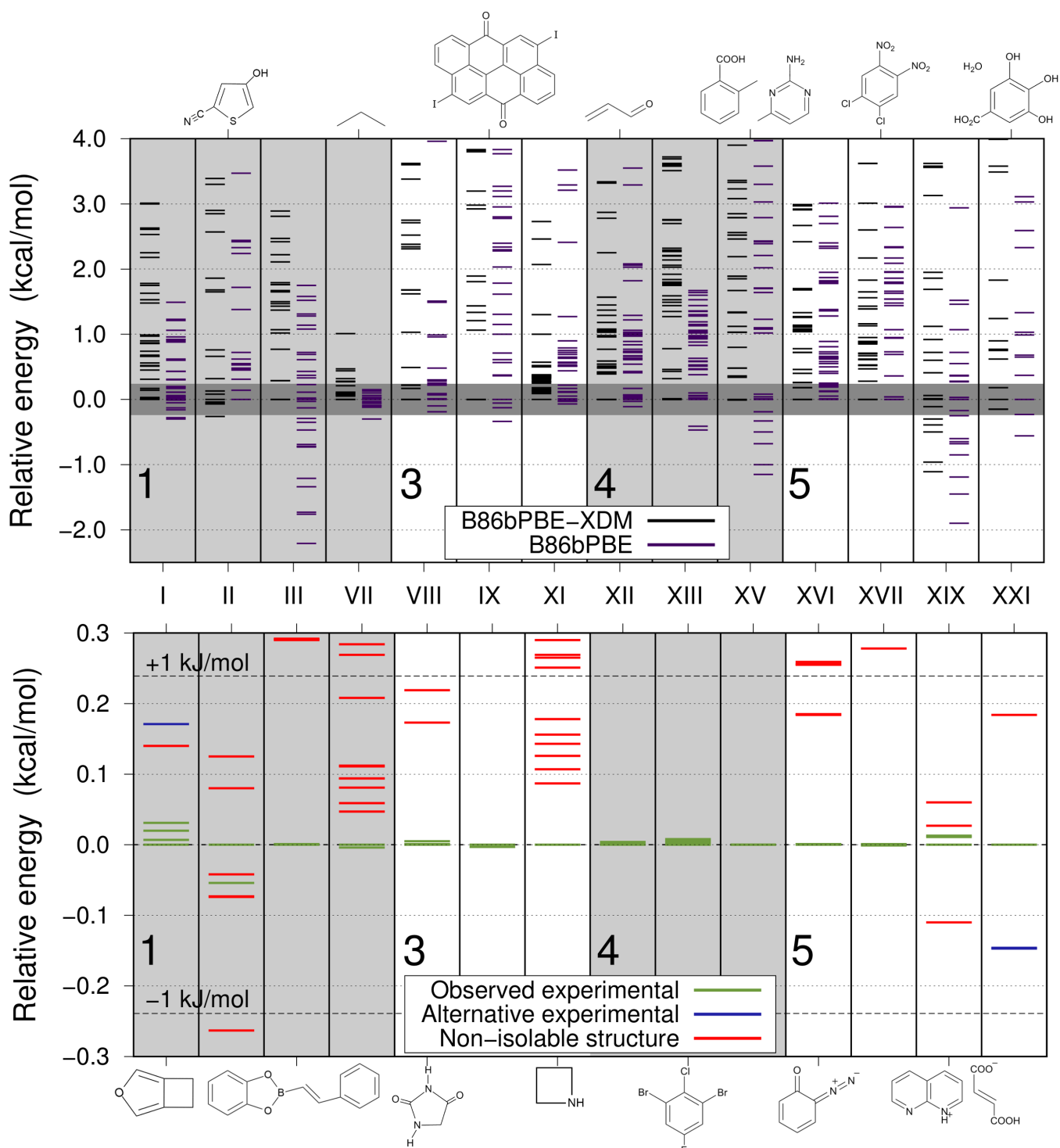
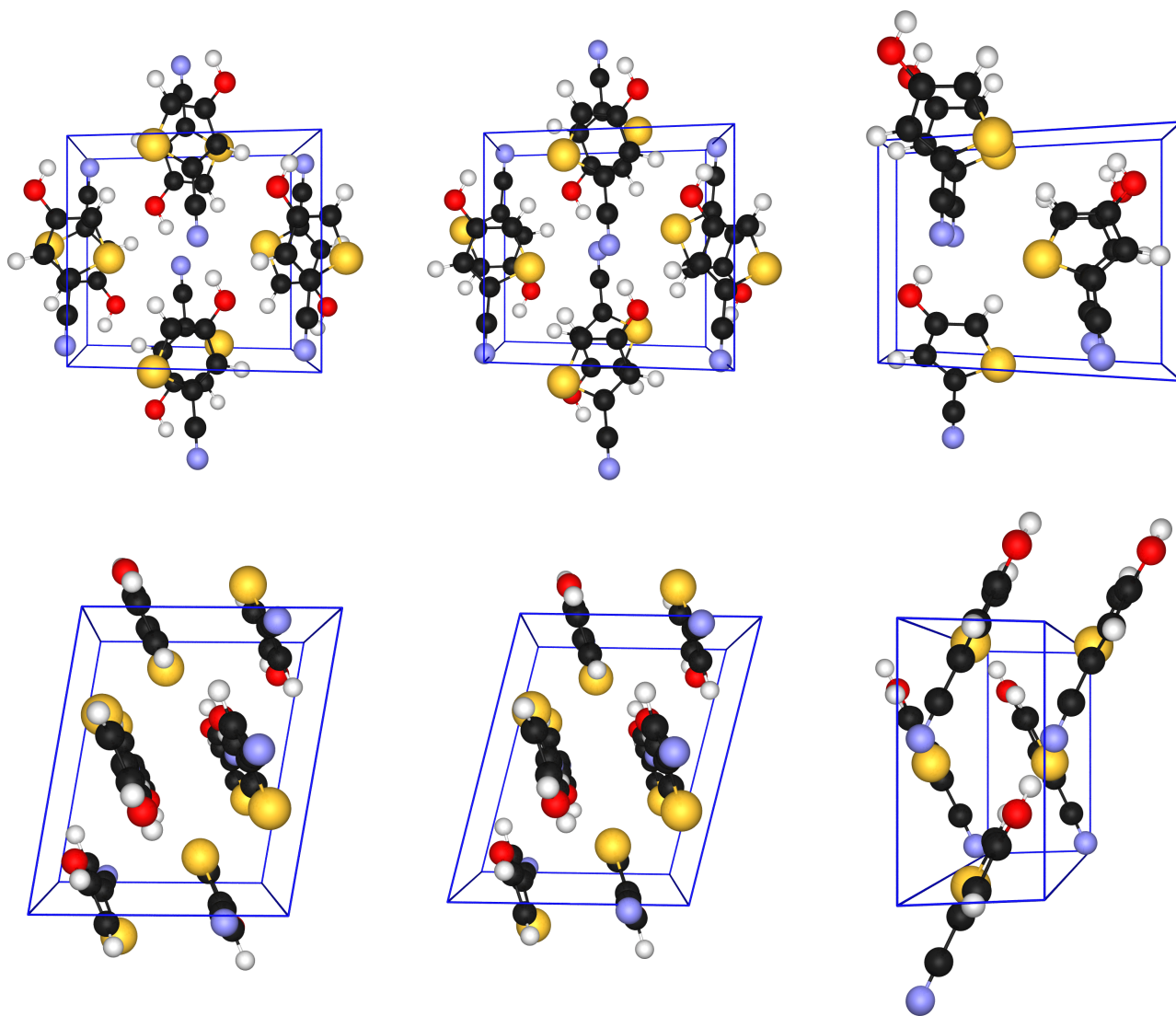


Figure 2: Comparison of predicted structures for compound II. Shown are the experiment structure (left), the very similar Verwer-2 structure (center), and the Verwer-3 structure, which has the lowest energy with DFT-XDM (right). Two different views are shown for each crystal, one per row.



seen for compound I, the potential-energy surface for the experimental form is very flat with respect to the “slip” between the stacked rings, as shown in Figure 2. As such, relaxations for the experimental structure and the Verwer-2 structure, which was deemed to match experiment according to analysis of the molecular packing,¹ converged to yield slightly different unit-cell volumes and energies. The DFT-XDM energies differ by only 0.05 kcal/mol per molecule in favour of Verwer-2. Additional calculations using the Nudged Elastic Band (NEB) approach and the Climbing Image technique^{61,69,70} demonstrated that interconversion between these two structures is actually bar-

rierless, so these should be properly viewed as equivalent. The geometry optimization appears to converge to the slightly higher-energy structure due to the flatness of the potential.

Even taking Verwer-2 as our reference, DFT-XDM identifies Verwer-3, also shown in Figure 2, as lying 0.25 kcal/mol per molecule lower in energy. This crystal is characterized by a wine-rack motif, rather than the tilted rows of π -stacked molecules seen in the experimental/Verwer-2 packing arrangement. Given the small energy difference, it is possible that the vibrational free-energy contribution is sufficient to preferentially stabilize the experimental structure. Thankfully both unit cells

for the compound are quite small (44 atoms for experiment versus 22 atoms for Verwer-3), so it was possible to determine the extent of the free-energy correction using a quasi-harmonic procedure analogous to the one used in our previous benchmark study.⁴⁴

Phonon calculations were performed using the finite displacement method (as implemented in the phonopy program⁷¹) on the experimental, Verwer-2, and Verwer-3 crystal structures. For each crystal, four negative pressures were considered: 0, -0.25 , -0.5 , and -0.75 GPa, and the equilibrium geometries, energies, and phonon frequencies at Γ under those pressures were calculated. The volume-dependent vibrational free energy contribution was fitted to a second-degree polynomial and the thermal pressure determined from its derivative at the equilibrium volume, in a procedure analogous to the one we used in the past for the C21 set.⁴⁴ Finally, the vibrational contribution is interpolated from the free energy *vs.* pressure curve. Naturally, we are limited to this rough estimate because of computational cost constraints—higher quality calculations necessitate a proper reciprocal-space sampling (see Ref. 23 and references therein).

Including this quasi-harmonic thermal correction, it was found that the experimental structure is indeed more stable than Verwer-3 by 0.58 kcal/mol per molecule. While the correct energy ranking is now recovered, this indicates that thermal contributions may be quite important in some cases, as recently pointed out by Heit and Beran.⁷² Indeed the finding that thermal effects are needed to recover the correct energy ranking for 1/11 molecules is statistically consistent with the work of Nyman and Day, who showed that thermal effects change the energy ordering for 9% of organic compounds.²³

The results for the rest of the compounds in BT1 and BT3 illustrate the advantage in accuracy B86bPBE-XDM has over the force fields used in early blind tests. This increased performance comes at a quite higher computational cost, making a two-step approach to energy ranking (pre-screening with a force field and final ranking with XDM) very attractive. Of the considered compounds (III, VII, VIII, IX, and

XI), force-field approaches had success in only four instances: Mooij-1 and van Eijck-1 for III, Mooij-1 for VII, and Day-1 for IX. In contrast, B86bPBE-XDM predicted experiment to be the global energy minimum for all five compounds. Some of the force-field failures could be ascribed to deficiencies in the candidate generation algorithm¹ (like, for instance, the treatment of torsional flexibility in III). In other cases, the molecule was not among the typical moieties for which the force field were parametrized (XI), or the molecule contained unfamiliar atoms (such as iodine in compound IX).^{1,3}

Another observation derived from our results is that a large number of candidates were found within a small energy range for most of these five crystals.^{1,3} Although a more exhaustive ranking using the extended list would be desirable, Figure 1 shows that B86bPBE-XDM has a discriminating effect on the proposed candidates compared to the blind test predictions and to the non-dispersion corrected B86bPBE results. In compound III, for instance, no candidates are found within the polymorphism stability region (± 1 kJ/mol²³). The separation effect caused by the dispersion correction seems to be stronger in polar systems and in compounds that can form hydrogen bonds. For hydrophobic systems like VII or XI, where the main contributor to binding is a non-directional non-specific interaction like dispersion, a number of structures are found within the polymorphism energy range. However, B86bPBE-XDM is still accurate enough to identify the experimental structure as the one with lowest lattice energy.

Appreciable discussion in the third blind test involved compound XI, azetidine. The existence of two molecules in the asymmetric unit, the relatively uncommon structure (a four-member ring) and the dominant character of dispersion effects (that necessitate higher accuracy, according to the preceding discussion) prevented any of the participants from predicting the correct structure.³ Many candidate structures were found within a very small energy range, and some participants found that a symmetry breaking from the experimental $P2_1/c$ space group to the $P\bar{1}$ subgroup lowered the

energy of the system. This raised the question of whether the experimentally observed $P2_1/c$ structure was an energy minimum or the thermal average of competing $P\bar{1}$ minima. The symmetry breaking argument is refuted by our B86bPBE-XDM results which not only predict the experimental structure as the global minimum, but also preserve the $P2_1/c$ symmetry of the crystal arrangement.

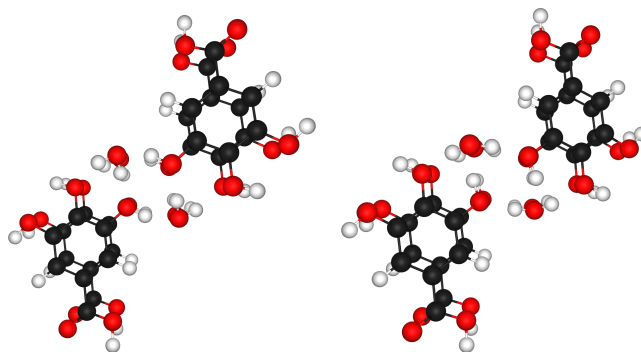
The single-molecule crystals in BT4 and BT5^{4,5} (XII, XIII, XVI, and XVII) were correctly predicted by Neumann *et al.* using a dispersion-corrected DFT methodology similar to the one presented in this article (and with a comparably high computational cost). For some of them, other groups were successful in their predictions as well (XII: Ammon-2, Boerrigter-1, and Schweizer-2; XIII: Ammon-2, Day-1, and Price-1; XVI: van Eijck-2; XVII: Price-2). In all cases except XVI, only the experimental crystal structure is found within the polymorphism energy range.

Co-Crystals

The DFT-XDM and base-functional results for the co-crystals are summarized in Table 2 and Figure 1. From the results in the table, DFT-XDM correctly identifies the stable structure for two of the three co-crystals, but favours an incorrect structure for the salt. The prediction of 1:1 co-crystal structures is challenging for the candidate generation algorithm because of the increased number of degrees of freedom (see Ref. 4 and references therein). However, there is nothing particularly more difficult about the energy ranking in these systems compared to the single-molecule crystals, and B86bPBE-XDM, as well as the methods of Neumann *et al.* and of van Eijck, correctly predicted the structure of compound XV.⁴

For gallic acid monohydrate (XXI), two stable polymorphs had been characterized experimentally prior to the blind test.^{73,74} Two additional forms had been submitted as CSP candidates, but form three had a disordered hydrogen-bonding network and was therefore deemed unsuitable, so form four was used as the single target of the blind test.^{75,76} This form is charac-

Figure 3: Experimental structure for the hydrate (left) and the structure predicted to be lowest in energy with dispersion-corrected DFT (right), which differ only in the hydrogen positions.

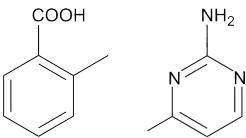
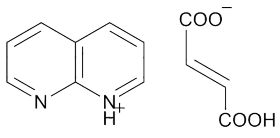
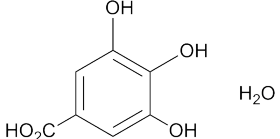


terized by an absence of carboxylic acid dimers and instead involves hydrogen bonds from the carboxylic acid moiety to both water and the polyphenol groups.

The polymorphism in compound XXI was subsequently studied computationally and experimentally by Braun *et al.*⁷ The authors found that gallic acid, both in its anhydrate and hydrated structures, presents extensive polymorphism. In particular, three anhydrates and five hydrates were experimentally determined, and it was shown that more than 20 other solvates are experimentally obtainable as well. The occurrence of each individual form depends on experimental conditions, mainly temperature and humidity.⁷ To assess B86bPBE-XDM in this compound, we restricted our calculations to the submitted crystal structures similar to form 4 of the monohydrate (no carboxylic acid dimers) to avoid predictions that would correspond to one of the other stable forms.

The situation for this crystal is complicated further because the experimental X-ray structure does not identify the hydrogen positions. Different structures can be obtained depending on the proton ordering.⁵ Two structures (Price-1 and van Eijck-2) were found to match the experimental heavy-atom packing, but not the hydrogen positions. With DFT-XDM, these two structures were predicted to be degenerate and this H-bonding arrangement is slightly more stable than the experimental structure by 0.15 kcal/mol per molecule. The different H-

Table 2: Summary of XDM-corrected and base density-functional results for the co-crystals. The blind test (“BT”) in which the crystal structures were reported is indicated, and the roman numeral is the compound identifier in the blind test articles. The ✓ symbol indicates that the experimental crystal structure was correctly predicted to be the lowest in energy. The ✗ symbol indicates that at least one other polymorph was predicted to be lower in energy than the experimental structure. The difference in energy between the most stable candidate and the experimental structure is also shown with and without XDM (ΔE_{XDM} and ΔE_{base} , both in kcal/mol). The latter was calculated at the B86bPBE-XDM equilibrium geometry.

Compound	Number	BT	XDM	Base	ΔE_{XDM}	ΔE_{base}
	XV	4	✓	✗	—	-1.19
	XIX	5	✗	✗	-1.11	-1.90
	XXI	5	✓ ^a	✗	-0.15	-0.56

^a The lowest-energy structure differs from experiment only in the hydrogen-atom positions, which cannot be assigned uniquely from X-ray data.

bonding motifs are shown in Figure 3.

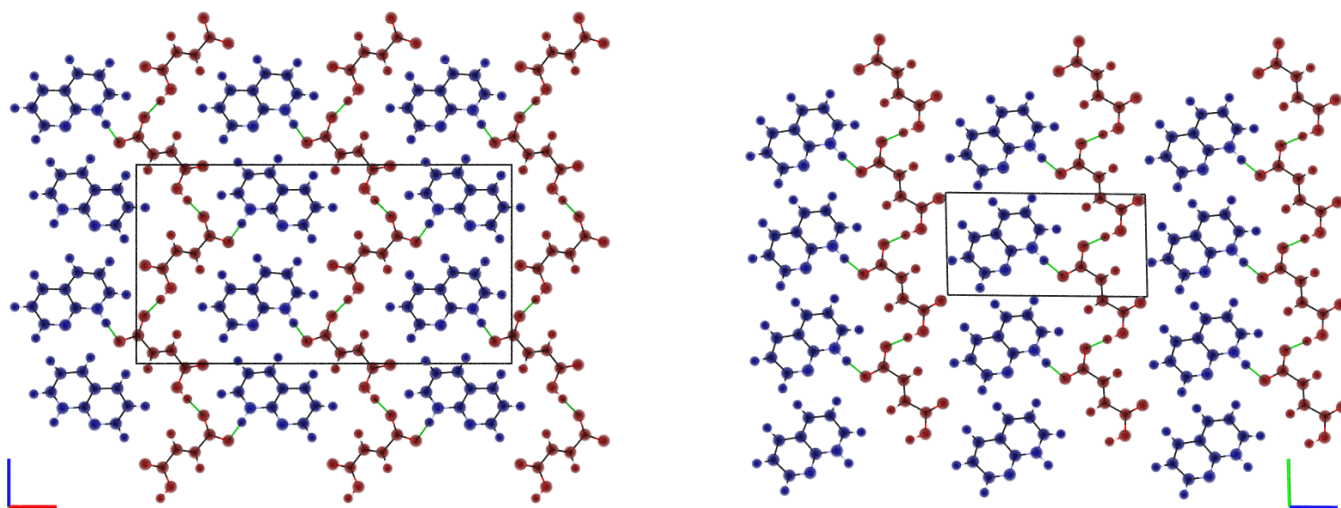
Finally, turning to the organic salt (XIX), it is not expected that the present methodology would accurately predict the minimum-energy structure, due to the inherent charge-transfer error in the base functional.^{49–52} Generalized-gradient approximation (GGA) functionals, as used in the present work, are well-known to preferentially stabilize electron distributions with fractional, rather than integer, charges.^{53,54,77–79} This is the case for the salt, where the charges on each monomer are found to be ± 0.82 , according to Bader analysis⁸⁰ of the B86bPBE-XDM electron density, evidencing the strong charge-transfer component in this crystal.

DFT-XDM matches the previous DFT ranking²⁵ and predicts the Neumann-1 structure to be the most stable, lying 1.1 kcal/mol lower in energy than experiment. This difference is almost entirely due to the base functional alone, rather than originating from a difference in dispersion stabilization, an effect sim-

ilar to our observations for halogen-bonded dimers.⁵³ Delocalization error is expected to affect hydrogen-bonded systems as well, although to a lesser extent.⁵⁴ The experimental and DFT-XDM minimum-energy structures for the salt are shown in Figure 4. They both consist of alternating rows of cations and anions, but differ in the H-bonding arrangements. In the Neumann-1 structure, all the $\text{NH}^+ - \text{COO}^-$ H-bonds occur along the same adjacent row but, in the experimental structure, successive cations form H-bonds to anions in opposite rows. The interlayer packing of Neumann-1 matches the experimental structure in all other respects, so it is this difference in H-bonding that determines the relative ordering. Further analysis of the Bader charges reveals that the atomic charges for the hydrogen-bond donors in the Neumann-1 structure are smaller in magnitude and farther from integer values, which justifies its greater stability, relative to the experimental structure.

In principle, an energy ranking of the same

Figure 4: Experimental structure for the organic salt (left) and the structure predicted to be lowest in energy with dispersion-corrected DFT (right). The cations are shown in blue and the anions in red to highlight the differences between structures. Unit cells are represented by boxes.



accuracy as the other compounds could be obtained for the organic salt, provided a base functional that minimizes delocalization error is employed. Although delocalization error is at present an unsolved problem in DFT, hybrid functionals that incorporate 50% of exact exchange and range-separated functionals (such as LC- ω PBE) have demonstrated success in similar systems, such as halogen-bonded dimers or the beyond-3-body interactions in HF clusters.^{53,54} However, application of these methods to molecular crystals is currently not computationally feasible.

Equilibrium geometries

Table 3 compares the geometries submitted by the blind test participants and the B86bPBE-XDM equilibrium geometries with the experimental X-ray structures. Two similarity indices are used. The “POW” adimensional index is a similarity measure based on the overlap between calculated powder diffraction patterns using cross-correlated weighting functions⁸² as implemented in *critic2*.⁶³ The other index (“RMSD₁₅”) is similar to the one used in recent blind tests and implemented in the *mercury* program.⁸¹ This index is calculated by building a molecular environment containing 15 molecules for the two crystals, and then calcu-

lating the RMSD between the two environments in the situation of maximum overlap. For both indices, zero indicates a perfect match. Being based on powder diffraction spectra, the POW index is more sensitive to changes in the cell shape and dimensions than RMSD₁₅, while the opposite is true about atomic displacements in the molecular motif.

In general, the B86bPBE-XDM values show good agreement with experiment, although it is outperformed by at least one of the force fields for most compounds. The geometries calculated by van Eijck et al. seem to be in particularly good agreement with the X-ray results. The geometries predicted by Neumann et al. using dispersion-corrected DFT are also in excellent agreement with experiment, with essentially matching powder diffraction patterns. However, B86bPBE-XDM obtains better RMSD₁₅ results than Neumann et al. except in compounds XIII, for which they obtain the same RMSD₁₅, and XV, which is 0.005 Å higher.

The results in Table 3 should be interpreted with care. The B86bPBE-XDM geometries, as well as many of the structures submitted by the participants, are minima of the electronic energy and are not directly comparable to the experimental geometries because of thermal expansion effects.⁴⁴ For instance, Heit and Beran have reported a systematic underestimation of

Table 3: Similarity indices comparing the DFT-XDM equilibrium structure (“B86bPBE-XDM”) and the structures submitted by the blind test participants to the corresponding experimental structures. The powder diffraction index (“POW”) computed using the critic2 program⁶³ and the RMSD index (“RMSD₁₅”, in Å) computing using the mercury program⁸¹ are shown. The N_c column shows the number of matching molecules calculated by mercury (out of a total of 15).

	Structure	POW	RMSD ₁₅	N_c		Structure	POW	RMSD ₁₅	N_c
I	B86bPBE-XDM ^a	0.1225	0.077	15	XII	Schweizer-2	0.2362	0.178	15
I	Gavezzotti-1 ^a	0.1599	0.204	15	XIII	B86bPBE-XDM	0.0306	0.080	15
I	van Eijck-3 ^{a,b}	0.1557	0.189	11	XIII	Ammon-1	0.0925	0.358	15
I	Verwer-1 ^a	0.2603	0.195	15	XIII	Ammon-2 ^d	0.1879	0.500	15
I	Williams-1 ^a	0.3296	0.298	15	XIII	Day-1	0.0310	0.157	15
II	B86bPBE-XDM	0.0646	0.074	15	XIII	Neumann-1	0.0210	0.080	15
II	Verwer-2 ^c	0.1608	0.591	15	XIII	Price-1	0.0560	0.143	15
III	B86bPBE-XDM	0.1317	0.117	15	XV	B86bPBE-XDM	0.0935	0.083	15
III	Mooij-1 ^d	0.5640	0.91	10	XV	Neumann-1	0.0089	0.078	15
III	van Eijck-1	0.0801	0.223	15	XV	van Eijck-3 ^f	0.4344	n/a	0
VII	B86bPBE-XDM	0.3357	0.495	10	XVI	B86bPBE-XDM	0.0616	0.127	15
VII	Mooij-1	0.3409	0.133	9	XVI	Neumann-1	0.0462	0.157	15
VIII	B86bPBE-XDM	0.2332	0.175	15	XVI	van Eijck-2	0.0943	0.247	15
VIII	Day-1	0.5161	0.326	15	XVII	B86bPBE-XDM	0.0029	0.025	15
VIII	van Eijck-1	0.1554	0.326	15	XVII	Neumann-1	0.0029	0.045	15
VIII	Facelli-2 ^e	—	—	—	XVII	Price-2	0.0186	0.134	15
VIII	Pantelides-1 ^e	—	—	—	XIX	B86bPBE-XDM	0.1336	0.144	15
IX	B86bPBE-XDM	0.1796	0.183	15	XIX	Neumann-3	0.0381	0.150	15
IX	Day-1	0.0159	0.076	15	XIX	van Eijck-2	0.0558	0.218	15
XI	B86bPBE-XDM	0.2711	0.125	15	XXI	B86bPBE-XDM ^g	0.0524	0.132	15
XII	B86bPBE-XDM	0.2711	0.115	15	XXI	Price-3 ^{g,h}	0.3570	0.583	15
XII	Ammon-2	0.3632	0.178	15	XXI	van Eijck-1 ^{g,h}	0.0259	0.219	15
XII	Boerrigter-1	0.1693	0.157	15	XXI	van Eijck-2 ^{g,h}	0.3868	0.583	15
XII	Neumann-1	0.0366	0.128	15					

^a Compared against the *Pbca* polymorph.

^b Converged to a structure similar to experiment but with a slight tilt.

^c Converged to a structure similar to experiment but slightly displaced in the molecular plane.

^d Was not marked as correct in the blind test, but converged to the experimental structure upon geometry relaxation using B86bPBE-XDM.

^e Structure not given in the SI.

^f Differs from experiment by methyl-group rotation.

^g Compared against experimental form 4.

^h Heavy atoms match, different proton ordering.

cell volumes of 5–10% on average caused by neglect of vibrational effects.⁷²

The impact of missing thermal expansion on the similarity indices in Table 3 can be estimated easily by comparing the equilibrium and thermally expanded structures for the crystals in the C21 set reported in Ref. 44. In those crystals, thermal expansion has been modeled by relaxing the equilibrium geometry of the crystal under a (negative) thermal pressure determined from the calculated vibrational free energies at different cell volumes. The average POW index between the 21 equilibrium and thermally expanded crystal pairs is 0.254, which is in the range of the disagreement between B86bPBE-XDM and other methods with the experimental structure in Table 3. The mean RMSD₁₅ deviation for the 21 crystal pairs is 0.078 Å, also in the range of the observed differences in Table 3. In addition, the B86bPBE-XDM volumes of all crystals except for XVII are underestimated, with a root-mean-square volume difference of 3.2%. The agreement with the experimental XVII structure in Table 3 is either the result of an unusually small thermal expansion or of an error cancellation between an overestimated B86bPBE-XDM equilibrium volume and the neglect of vibrational effects.

Conclusions

This work presents a systematic benchmark of DFT-XDM for energy ranking of molecular crystals, which is the essential final step in any crystal structure prediction method. The B86bPBE density functional combined with the exchange-hole dipole moment dispersion model (XDM) was found to reliably identify the experimental structure as the lowest-energy candidate for all but one of 14 planar compounds and co-crystals from the CSP blind tests. Further investigation of the suitability of DFT-XDM for energy ranking for the non-planar and flexible-molecule compounds of the blind tests, where more complicated effects may be at play, are planned. Based on the current results, DFT-XDM is an excellent method for energy ranking of organic molecular crystals. In particular,

B6BPBE-XDM holds promise for application to crystal-structure prediction of energetic materials, organic electronics, or active pharmaceutical ingredients.

Supporting Information Available: Tables of the relative energies and crystal volumes per molecule computed for each submitted candidate structure. This material is available free of charge via the Internet at <http://pubs.acs.org/>.

Acknowledgement The authors thank Compute Canada (Westgrid) and the Spanish Malta/Consolider initiative, award number CSD2007-00045 for computational resources. ERJ thanks the National Science and Engineering Research Council of Canada (NSERC) and the National Science Foundation (NSF), award number CHE-1300686, for funding.

References

- (1) Lommerse, J. P. M. et al. A test of crystal structure prediction of small organic molecules. *Acta Cryst.* **2000**, *B58*, 647–661.
- (2) Motherwell, W. D. S. et al. Crystal structure prediction of small organic molecules: a second blind test. *Acta Cryst.* **2002**, *B58*, 647–661.
- (3) Day, G. M. et al. A third blind test of crystal structure prediction. *Acta Cryst.* **2005**, *B61*, 511–527.
- (4) Day, G. M. et al. Significant progress in predicting the crystal structures of small organic molecules - a report on the fourth blind test. *Acta Cryst.* **2009**, *B65*, 107–125.
- (5) Bardwell, D. A. et al. Towards crystal structure prediction of complex organic compounds – a report on the fifth blind test. *Acta Cryst.* **2011**, *B67*, 535–551.
- (6) Maddox, J. Crystals from first principles. *Nature* **1988**, *335*, 201.

- (7) Braun, D. E.; Bhardwaj, R. M.; Florence, A. J.; Tocher, D. A.; Price, S. L. Complex Polymorphic System of Gallic Acid Five Monohydrates, Three Anhydrides, and over 20 Solvates. *Cryst. Growth Des.* **2013**, *13*, 19–23.
- (8) Price, S. L. Why don't we find more polymorphs? *Acta Crystallogr. Sect. B: Struct. Sci.* **2013**, *69*, 313–328.
- (9) Cruz-Cabeza, A. J.; Reutzel-Edens, S. M.; Bernstein, J. Facts and fictions about polymorphism. *Chem. Soc. Rev.* **2015**, *44*, 8619–8635.
- (10) Reilly, A. M.; Tkatchenko, A. Role of Dispersion Interactions in the Polymorphism and Entropic Stabilization of the Aspirin Crystal. *Phys. Rev. Lett.* **2014**, *113*, 055701.
- (11) Morissette, S. L. et al. High-throughput crystallization: polymorphs, salts, cocrystals and solvates of pharmaceutical solids. **2004**, *56*, 275–300.
- (12) Singhai, D.; Curatolo, W. Drug polymorphism and dosage form design: a practical perspective. *Adv. Drug Deliv. Rev.* **2004**, *56*, 335–347.
- (13) Pudipeddi, M.; Serajuddin, A. T. M. Trends in solubility of polymorphs. *J. Pharm. Sci.* **2005**, *94*, 929–939.
- (14) Blagden, N.; de Matas, M.; Gavan, P. T.; York, P. Crystal engineering of active pharmaceutical ingredients to improve solubility and dissolution rates. *Adv. Drug Deliv. Rev.* **2007**, *59*, 617–630.
- (15) Bauer, J. et al. Ritonavir: An Extraordinary Example of Conformational Polymorphism. *Pharm. Res.* **2001**, *18*, 859–866.
- (16) Millar, D. I. et al. The crystal structure of -RDX an elusive form of an explosive revealed. *Chem. Commun.* **2009**, 562–564.
- (17) Bolton, O.; Matzger, A. J. Improved Stability and Smart-Material Functionality Realized in an Energetic Cocrystal. *Angew. Chem.* **2011**, *50*, 8960–8963.
- (18) Troisi, A.; Orlandi, G. Band structure of the four pentacene polymorphs and effect on the hole mobility at low temperature. *J. Phys. Chem. B* **2005**, *109*, 1849–1856.
- (19) Pfattner, R. et al. High-Performance Single Crystal Organic Field-Effect Transistors Based on Two Dithiophene-Tetrathiafulvalene (DT-TTF) Polymorphs. *Adv. Mater.* **2010**, *22*, 4198.
- (20) Jurchescu, O. D. et al. Effects of polymorphism on charge transport in organic semiconductors. *Phys. Rev. B* **2009**, *80*, 085201.
- (21) Reilly, A. M. et al. Report on the sixth blind test of organic crystal structure prediction methods. *Acta Cryst. B* **2016**, *72*, 439–459.
- (22) Gavezzotti, A.; Filippini, G. Polymorphic Forms of Organic Crystals at Room Conditions: Thermodynamic and Structural Implications. **1995**, *117*, 12299–12305.
- (23) Nyman, J.; Day, G. M. Static and lattice vibrational energy differences between polymorphs. *CrystEngComm* **2015**, *17*, 5154.
- (24) Hylton, R. K. et al. Are the Crystal Structures of Enantiopure and Racemic Mandelic Acids Determined by Kinetics or Thermodynamics? *J. Am. Chem. Soc.* **2015**, *137*, 11095–11104.
- (25) Neumann, M. A.; Leusen, F. J. J.; Kendrick, J. A Major Advance in Crystal Structure Prediction. *Angew. Chem. Int. Ed.* **2008**, *47*, 2427–2430.
- (26) Neumann, M. A.; Perrin, M.-A. Energy ranking of molecular crystals using density functional theory calculations and an empirical van der Waals correction. *J. Phys. Chem. B* **2005**, *109*, 15531–15541.

- (27) Brandenburg, J. G.; Grimme, S. Organic crystal polymorphism: a benchmark for dispersion corrected mean field electronic structure methods. *Acta Cryst. B* **2016**, *72*, 502–513.
- (28) Wen, S. H.; Beran, J. O. Crystal Polymorphism in Oxalyl Dihydrazide: Is Empirical DFT-D Accurate Enough? *J. Chem. Theory Comput.* **2012**, *8*, 2698–2705.
- (29) Presti, D.; Pedone, A.; Menziani, M. C.; Civalleri, B.; Maschio, L. Oxalyl dihydrazide polymorphism: a periodic dispersion-corrected DFT and MP2 investigation. *CrystEngComm* **2014**, *16*, 102–109.
- (30) Taylor, C. R.; Bygrave, P. J.; Hart, J. N.; Allan, N. L.; Manby, F. R. Improving density functional theory for crystal polymorph energetics. *Phys. Chem. Chem. Phys.* **2012**, *14*, 7739–7743.
- (31) Marom, N. et al. Many-Body Dispersion Interactions in Molecular Crystal Polymorphism. **2013**, *52*, 6629–6632.
- (32) Wahlberg, N.; Clochon, P.; Petrlicek, V.; Madsen, A. Polymorph Stability Prediction: On the Importance of Accurate Structures: A Case Study of Pyrazinamide. *Cryst. Growth Des.* **2014**, *14*, 381–388.
- (33) Brandenburg, J. G.; Maas, T.; Grimme, S. Benchmarking DFT and semiempirical methods on structures and lattice energies for ten ice polymorphs. *J. Chem. Phys.* **2015**, *142*, 124104.
- (34) Cruz-Cabeza, A. J.; Reutzel-Edens, S. M.; Bernstein, J. Facts and fictions about polymorphism. *Chem. Soc. Rev.* **2015**, *44*, 8619–8635.
- (35) Grimme, S. Semiempirical GGA-type density functional constructed with a long-range dispersion correction. *J. Comp. Chem.* **2006**, *27*, 1787–1799.
- (36) Grimme, S.; Antony, J.; Ehrlich, S.; Krieg, H. A consistent and accurate ab initio parametrization of density functional dispersion correction (DFT-D) for the 94 elements H-Pu. *J. Chem. Phys.* **2010**, *132*, 154104.
- (37) Dion, M.; Rydberg, H.; Schröder, E.; Langreth, D. C.; Lundqvist, B. I. Van der Waals density functional for general geometries. *Phys. Rev. Lett.* **2004**, *92*, 246401.
- (38) Lee, K.; Murray, É. D.; Kong, L.; Lundqvist, B. I.; Langreth, D. C. Higher-accuracy van der Waals density functional. *Phys. Rev. B* **2010**, *82*, 081101.
- (39) Tkatchenko, A.; Scheffler, M. Accurate molecular van der Waals interactions from ground-state electron density and free-atom reference data. *Phys. Rev. Lett.* **2009**, *102*, 073005.
- (40) Tkatchenko, A.; DiStasio, R. A.; Car, R.; Scheffler, M. Accurate and Efficient Method for Many-Body van der Waals Interactions. *Phys. Rev. Lett.* **2012**, *108*, 236402.
- (41) Becke, A. D.; Johnson, E. R. Exchange-hole dipole moment and the dispersion interaction revisited. *J. Chem. Phys.* **2007**, *127*, 154108.
- (42) Otero-de-la Roza, A.; Johnson, E. R. Van der Waals Interactions in Solids Using the Exchange-Hole Dipole Moment Model. *J. Chem. Phys.* **2012**, *136*, 174109.
- (43) Otero-de-la Roza, A.; Johnson, E. R. Non-Covalent Interactions and Thermochemistry using XDM-Corrected Hybrid and Range-Separated Hybrid Density Functionals. *J. Chem. Phys.* **2013**, *138*, 204109.
- (44) Otero-de-la Roza, A.; Johnson, E. R. A benchmark for non-covalent interactions in solids. *J. Chem. Phys.* **2012**, *137*, 054103.

- (45) Otero-de-la Roza, A.; Cao, B. H.; Price, I. K.; Hein, J. E.; Johnson, E. R. Density-functional theory predicts the relative solubilities of racemic and enantiopure crystals. *Angew. Chem. Int. Ed.* **2014**, *53*, 7879–7882.
- (46) Beran, G. J. O. Modeling Polymorphic Molecular Crystals with Electronic Structure Theory. *Chem. Rev.* **2016**, *116*, 5567–5613.
- (47) Cutini, M. et al. Assessment of Different Quantum Mechanical Methods for the Prediction of Structure and Cohesive Energy of Molecular Crystals. *J. Chem. Theory Comput.* **2016**, *12*, 3340–3352.
- (48) Nyman, J.; Pundyke, O. S.; Day, G. M. Accurate force fields and methods for modelling organic molecular crystals at finite temperatures. *Phys. Chem. Chem. Phys.* **2016**, *18*, 15828–15837.
- (49) Zhang, Y.; Wang, Y. A Challenge for Density Functionals: Self-Interaction Error Increases for Systems with a Noninteger Number of Electrons. *J. Chem. Phys.* **1998**, *109*, 2604–2608.
- (50) Tozer, D. J. Relationship Between Long-Range Charge-Transfer Excitation Energy Error and Integer Discontinuity in Kohn–Sham Theory. *J. Chem. Phys.* **2003**, *119*, 12697–12699.
- (51) Ruzsinszky, A.; Perdew, J. P.; Csonka, G. I.; Vydrov, O. A.; Scuseria, G. E. Spurious fractional charge on dissociated atoms: Pervasive and resilient self-interaction error of common density functionals. *J. Chem. Phys.* **2006**, *125*, 194112.
- (52) Cohen, A. J.; Mori-Sánchez, P.; Yang, W. Insights into Current Limitations of Density Functional Theory. *Science* **2008**, *321*, 792.
- (53) Otero-de-la Roza, A.; Johnson, E. R.; DiLabio, G. A. Halogen Bonding from Dispersion-Corrected Density-Functional Theory: the Role of Delocalization Error. *J. Chem. Theory Comput.* **2014**, *10*, 5436–5447.
- (54) Otero-de-la Roza, A.; DiLabio, G. A.; Johnson, E. R. Exchange-correlation effects for non-covalent interactions in density-functional theory. *J. Chem. Theory Comput.* **2016**, ASAP article, DOI: 10.1021/acs.jctc.6b00298.
- (55) Becke, A. On the large-gradient behavior of the density functional exchange energy. *J. Chem. Phys.* **1986**, *85*, 7184.
- (56) Perdew, J. P.; Burke, K.; Ernzerhof, M. Generalized gradient approximation made simple. *Phys. Rev. Lett.* **1996**, *77*, 3865.
- (57) Christian, M. S.; Otero-de-la-Roza, A.; Johnson, E. R. Surface Adsorption from the Exchange-Hole Dipole Moment Dispersion Model. *J. Chem. Theory Comput.* **2016**, *12*, 3305–3315.
- (58) Otero-de-la-Roza, A.; Johnson, E. R. Many-body dispersion interactions from the exchange-hole dipole moment model. *J. Chem. Phys.* **2013**, *138*, 054103.
- (59) Johnson, E. R. Dependence of dispersion coefficients on atomic environment. *J. Chem. Phys.* **2011**, *135*, 234109–234109.
- (60) Blöchl, P. E. Projector augmented-wave method. *Phys. Rev. B* **1994**, *50*, 17953.
- (61) Giannozzi, P. et al. QUANTUM ESPRESSO: a modular and open-source software project for quantum simulations of materials. *J. Phys.: Condens. Matter* **2009**, *21*, 395502.
- (62) Yu, M.; Trinkle, D. R. Accurate and efficient algorithm for Bader charge integration. *J. Chem. Phys.* **2011**, *134*, 064111–064111.
- (63) Otero-de-la Roza, A.; Johnson, E. R.; Luaña, V. Critic2: a program for real-space analysis of quantum chemical interactions in solids. *Comput. Phys. Commun.* **2014**, *185*, 1007–1018.

- (64) Braun, D. E.; McMahon, J. A.; Koztecki, L. H.; Price, S. L.; Reutzel-Edens, S. M. Contrasting Polymorphism of Related Small Molecule Drugs Correlated and Guided by the Computed Crystal Energy Landscape. *Crystal Growth & Design* **2014**, *14*, 2056–2072.
- (65) Gelbrich, T.; Braun, D. E.; Ellern, A.; Griesser, U. J. Four Polymorphs of Methyl Paraben: Structural Relationships and Relative Energy Differences. *Cryst. Growth Des.* **2013**, *13*, 1206–1217.
- (66) Wang, Y.; Perdew, J. P. Correlation hole of the spin-polarized electron gas, with exact small-wave-vector and high-density scaling. *Phys. Rev. B* **1991**, *44*, 13298.
- (67) Perdew, J. P. et al. Atoms, molecules, solids, and surfaces: Applications of the generalized gradient approximation for exchange and correlation. *Phys. Rev. B* **1992**, *46*, 6671–6687.
- (68) Wu, Q.; Yang, W. Empirical correction to density functional theory for van der Waals interactions. *J. Chem. Phys.* **2002**, *116*, 515.
- (69) Henkelman, G.; Uberuaga, B. P.; ; Jónsson, H. A climbing image nudged elastic band method for finding saddle points and minimum energy paths. *J. Chem. Phys.* **2000**, *113*, 9901–9904.
- (70) G, H.; Jónsson, H. Improved tangent estimate in the nudged elastic band method for finding minimum energy paths and saddle points. *J. Chem. Phys.* **2000**, *113*, 9978–9985.
- (71) Togo, A.; Tanaka, I. First principles phonon calculations in materials science. *Scr. Mater.* **2015**, *108*, 1–5.
- (72) Heit, Y. N.; Beran, G. How important is thermal expansion for predicting molecular crystal structures and thermochemistry at finite temperatures? *Acta Cryst. B* **2016**, *72*, 514–529.
- (73) Jiang, R.-W.; Ming, D.-S.; But, P. P. H.; Mak, T. C. W. Gallic acid monohydrate. *Acta Cryst.* **2000**, *C56*, 594–595.
- (74) Okabe, N.; Kyoyama, H.; Suzuki, M. Gallic acid monohydrate. *Acta Cryst.* **2001**, *E57*, o764–o766.
- (75) Clarke, H. D.; Arora, K. K.; Wojtas, L.; Zaworotko, M. J. Polymorphism in Multiple Component Crystals: Forms III and IV of Gallic Acid Monohydrate. *Cryst. Growth Des.* **2011**, *11*, 964–966.
- (76) Demirtas, G.; Degea, N.; Büyükgüngöra, O. A third monoclinic polymorph of 3,4,5-trihydroxybenzoic acid monohydrate. *Acta Cryst.* **2011**, *E67*, o1509–o1510.
- (77) Ruzsinszky, A.; Perdew, J. P.; Csonka, G. I.; Vydrov, O. A.; Scuseria, G. E. Density functionals that are one- and two- are not always many-electron self-interaction-free, as shown for H-2(+), He-2(+), LiH+, and Ne-2(+). *J. Chem. Phys.* **2007**, *126*, 104102.
- (78) Kim, M.-C.; Sim, E.; Burke, K. Understanding and reducing errors in density functional calculations. *Phys. Rev. Lett.* **2013**, *111*, 073003.
- (79) Johnson, E. R.; Otero de la Roza, A.; Dale, S. G. Extreme density-driven delocalization error for a model solvated-electron system. *J. Chem. Phys.* **2013**, *139*, 184116.
- (80) Bader, R. F. W. *Atoms in Molecules. A Quantum Theory*; Oxford University Press: Oxford, 1990.
- (81) Macrae, C. F. et al. Mercury CSD 2.0—new features for the visualization and investigation of crystal structures. *J. Appl. Cryst.* **2008**, *41*, 466–470.
- (82) de Gelder, R.; Wehrens, R.; Hageman, J. A. A generalized expression for the similarity of spectra: application to powder diffraction pattern classification. *J. Comput. Chem.* **2001**, *22*, 273–289.

Graphical TOC Entry

